

# Segmental Interaction Parameters of Binary Polymer Mixtures Evaluated from Binodals and from Surface-Segregation Profiles: Comparison with Small-Angle Neutron Scattering

Jacob Klein,\* Tobias Kerle,<sup>§</sup> Florian Zink,<sup>†</sup> and Erika Eiser<sup>‡</sup>

Department of Materials and Interfaces, Weizmann Institute of Science, Rehovot 76100, Israel

Received May 20, 1999; Revised Manuscript Received December 13, 1999

**ABSTRACT:** We compare segmental interaction parameters  $\chi_{AB}$  in binary polyolefin mixtures extracted from a fit to the binodal—as deduced from composition–depth profiling of thin films—with values extracted from small-angle neutron scattering (SANS), on the self-same blends. We find good quantitative agreement as regards both absolute values and compositional dependence of  $\chi_{AB}$ . We also compare values of  $\chi_{AB}$  obtained from composition–depth profiles of surface segregation in isotopic polystyrene mixtures with values deduced from SANS from these mixtures, and again we find good agreement between them. These results point to the use of thin-film composition–depth profiling, which is potentially a more accessible technique and requires far smaller quantities of material, as a convenient, accurate, and widely applicable alternative to SANS for measuring segmental interactions in binary polymer mixtures.

## 1. Introduction

A large number of investigations have been used to obtain structural or transport information in thin multicomponent polymer films (usually of binary mixtures or bilayers of two phases) by utilizing direct composition–depth profiling of such films. These have included the measurement of interdiffusion<sup>1–4</sup> and tracer diffusion<sup>5–7</sup> within the films, surface enrichment or complete wetting by one of the components from a binary polymer mixture,<sup>8–13</sup> surface-directed spinodal decomposition,<sup>14,15</sup> and interfacial structure between coexisting phases,<sup>16–18</sup> as well as the effect on these of the finite film thickness.<sup>19</sup> In a number of studies<sup>18,20–22</sup> the binodals for coexisting phases of binary A/B polymer mixtures were obtained via depth profiling in thin films: these were used to extract interaction parameters  $\chi_{AB}$  between the A and B segments. Here we focus more systematically on the use of composition–depth profiling to extract  $\chi_{AB}$  parameters for binary polymer mixtures. In particular, we compare our results with determination of interaction parameters for polymer blends using small-angle neutron scattering (SANS) via the random phase approximation (RPA). The purpose of this paper is to make explicit comparisons between the interaction parameters measured by these two very different methods for a number of identical binary mixtures: polyolefin mixtures for the case of the binodals, and an isotopic polystyrene mixture for the case of the surface-segregation profile. In section 2 we briefly note the basic ideas and the experimental approach and recall the interaction parameters from the binodals and their extraction from surface-segregation profiles from the earlier publications.<sup>22,23</sup> In section 3 we make a detailed comparison of these with values extracted from SANS studies, and in the final section we make some remarks concerning the applicability and limitations of the depth-profiling method. The comparison of the  $\chi_{AB}$  values reveals that

agreement between the two approaches is, within the experimental uncertainty, essentially quantitative. As thin-film composition–depth profiling is potentially a considerably more accessible technique, requiring also far smaller quantities of material, these results point to its use as a convenient, accurate, and widely applicable alternative to SANS for measuring segmental interactions in binary polymer blends.

## 2. Composition–Depth Profiling of Thin Films: Phase Coexistence and Surface Enrichment

The basic idea for extracting interaction parameters from thin-film composition–depth profiling is straightforward and is illustrated in parts a and b of Figure 1 for the case of mixtures in the two-phase and in the one-phase regimes, respectively. A binary polymer mixture (with an upper critical solution temperature  $T_c$ ) in a macroscopic bulk sample, when taken by cooling from a temperature  $T_1$  in the one-phase to a temperature  $T_2 < T_c$  in the two-phase regime (Figure 1a) will undergo demixing into two phases.

In time the different phases will tend to coalesce in order to reduce the interfacial energies (Ostwald ripening) and in principle should attain the configuration indicated in Figure 1a, top right, where an interface separates two macroscopic halves of the sample. The compositions  $\phi_1$  and  $\phi_2$  in the two halves can then be determined by chemical analysis; they define two points on the binodal, as shown in Figure 1a, corresponding to the temperature  $T_2$  on the temperature–composition phase coexistence diagram. In this way, by letting the mixture separate into two coexisting phases at different temperatures  $T < T_c$ , the full coexistence curve can be established. By fitting the data to the predictions of a standard model for the free energy of mixing as described below, the interaction parameter is readily extracted. In practice, the time for complete phase separation into two coexisting halves in a macroscopically thick sample (millimeters, say) of high molecular weight chains is essentially unattainable in practical times in most cases (indicated as “ $t \approx \infty$ ” in Figure 1a, top right). This is because of the sluggishness of the dynamics and the weakness of the driving surface-

<sup>†</sup> Present address: Department of Physics and Mathematical Physics, The University of Adelaide, Adelaide, SA 5005, Australia.

<sup>‡</sup> Present address: GDPC, Case 26, Université Montpellier 2, 34095 Montpellier Cedex 05, France.

<sup>§</sup> Present address: Materials Research Center on Polymers, University of Massachusetts, Amherst, MA 01003.

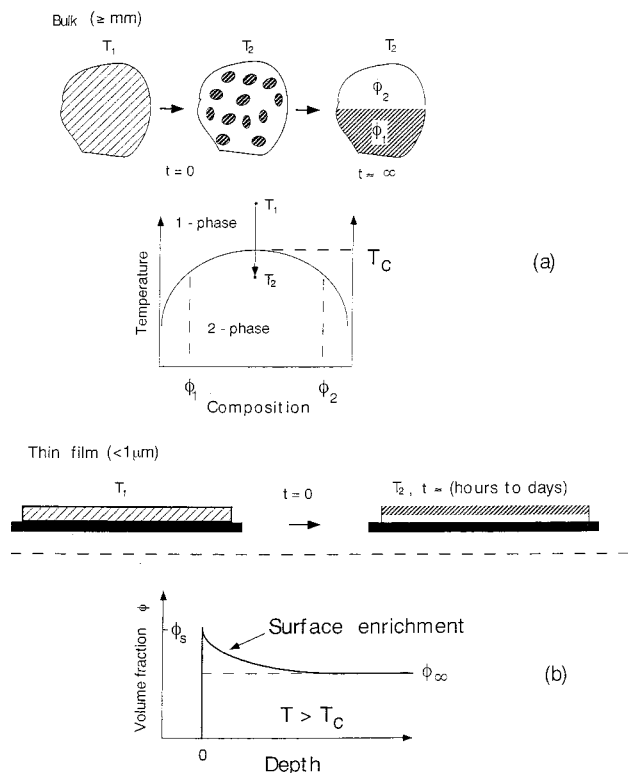


**Figure 1.** (a) Illustrating schematically the binodal construction from the values of the coexisting phase compositions at  $T < T_c$  in bulk samples (top) and in thin films (bottom). In the bulk, the time to attain coexistence in two distinct phases can be extremely long (noted as “ $t \approx \infty$ ”), while in sufficiently thin films it is accessible over laboratory times. (b) At temperatures  $T > T_c$  a surface-favored phase will enrich the surface and coexist with the bulk mixture composition, a situation which is attained in practical times in thin films. In both cases, fitting the binodal or the enrichment profile enables the segment interaction parameter  $\chi_{AB}$  to be extracted.

tension differences in polymer melts. In sufficiently thin films, however, as indicated in Figure 1a, bottom, complete separation into two layers of compositions  $\phi_1$  and  $\phi_2$  may occur readily in laboratory times of hours to days, as long as at the relevant temperatures of phase separation the polymer mixture is above its glass transition.

A different approach, useful for evaluating  $\chi_{AB}$  in a binary mixture in the one-phase regime ( $T > T_c$ ) for which one of the components has a preferential attraction to the surface, is to determine the composition–depth profile of the enriched component near that surface, as illustrated in Figure 1b. The decaying enrichment profile away from the surface may be fitted to the compositional variation predicted from a mean-field model incorporating the interaction parameter  $\chi_{AB}$ . In this way  $\chi_{AB}$  can be directly extracted.

Real-space composition–depth profiles in thin polymer films have been determined directly using several different ion beam techniques. These include Rutherford backscattering,<sup>1</sup> forward recoil scattering (FRoS),<sup>5,24–27</sup> dynamic secondary ion mass spectrometry (SIMS),<sup>10,28,29</sup> and nuclear reaction analysis (NRA) in both the resonant<sup>30</sup> and nonresonant mode.<sup>31</sup> In most of these techniques deuterium labeling of the species being profiled is necessary to provide the contrast.

In recent years we have used nonresonant NRA to investigate surface segregation and wetting in polymer mixtures in a wide range of conditions,<sup>11,13,32,33</sup> based

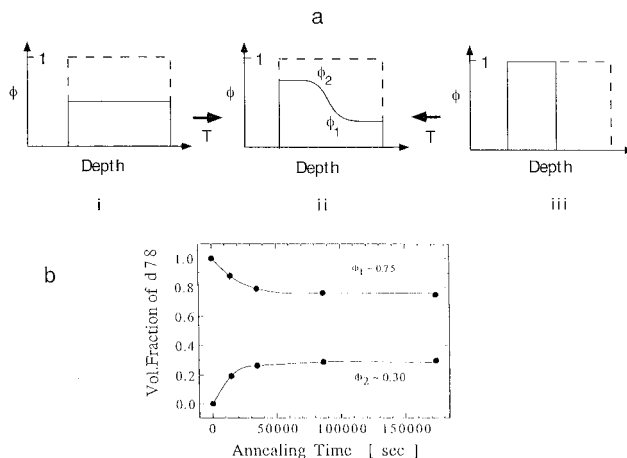


**Figure 2.** (a) Illustrating the two approaches for obtaining a profile of coexisting phases in thin films: in (i) the film is initially a single-phase mixture and demixes to the profile (ii) on being annealed at a temperature  $T < T_c$ . In (iii), a bilayer of the two pure components is allowed to interdiffuse at  $T < T_c$  until the coexisting profile (ii) is obtained. (b) The evolution with time of the coexisting compositions  $\phi_1$  and  $\phi_2$  obtained from composition–depth profiles in a thin film (e.g., (ii) above). The data are for the pair d78/h88 (see Table 1), taken at at 38 °C. In these conditions, where the interdiffusion between an initial bilayer configuration as in (iii) above takes place, the equilibrium coexisting values are attained within several hours (see also ref 21 for similar indications in high- $M$  polystyrene mixtures).

on  $\alpha$ -particle detection in the exothermic nuclear reaction  ${}^3\text{He} + {}^2\text{H} \rightarrow {}^4\text{He} + {}^1\text{H} + 18.352 \text{ MeV}$ . While convenient and straightforward to implement, the limited resolution of this approach did not in the past permit us to investigate the shape of the near-surface profile—of a phase enriched at that surface—in detail. Very recently, we improved the spatial resolution of this method<sup>34</sup> and can achieve an optimal resolution of some 3 nm (Gaussian half-width) at the sample surface. Such an enhanced resolution can be especially important in the measurement of the surface enrichment profiles, where an accurate determination of the profile shape is necessary to obtain a measure of the interaction parameter. The high spatial resolution is less important when determining coexisting phase compositions in a double-layer configuration, since there only the plateau values of the compositions are important. A high spatial resolution may however be useful even for the phase coexistence determinations, as it enables thinner bilayer films to be profiled, necessitating shorter times for equilibrium phase coexistence to be established.

For determination of the binodals of A/B mixtures, two approaches may be used, as illustrated schematically in the cartoon in Figure 2.

In the first approach, the components of the mixture (generally 50%/50%) are dissolved in a common solvent, and a thin film is spin-cast on a smooth solid substrate. The initial composition profile is indicated schematically in Figure 2a(i). On annealing at the required temperature  $T$ , the coexisting phases separate into two layers, as in Figure 2a(ii), with one phase (A-rich say) accumulating preferentially at the air surface. (The issue of layering of the phases parallel to the substrate is considered later.) In the second approach, a thin film of B is spin-cast on the substrate, and a similar layer of A is floated on water and mounted onto the B film. The initial composition profile is indicated schematically in Figure 2a(iii). On annealing at  $T$ , interdiffusion between

**Table 1. Molecular Parameters of Model Polyolefins<sup>a</sup>**

sample	% EE ( $x$ )	$N$	$f_D$
d52/h52	52	1510	0.34
d66/h66	66	2030	0.40
d78	78	1290	0.30
h88	88	1610	

<sup>a</sup> Molecular characteristics of the model polyolefins used in the present comparisons. The polymers have the structure  $([C_4H_8]_{1-x}[C_2H_3-(C_2H_5)]_x)_N$ , with different  $x$  values, where the ethyl (E:  $[C_4H_8]$ ) and the ethylethylene (EE:  $[C_2H_3-(C_2H_5)]$ ) monomers are distributed randomly on the chains. Within each pair, one of the components is partially deuterated (and labeled  $d_x$ , with  $x$  in %; the other—fully hydrogenated—component is labeled  $h_x$ ), to enable composition depth profiling by NRA. The characteristics of the components of the identical mixtures studied by the two methods are given in Table 1. The three pairs used were d52/h66, d66/h52, and d78/h88.  $f_D$  denotes the fractional deuteration of the deuterated sample (adapted from ref 22).

the two layers occurs, and bulk transport takes place until the coexisting compositions  $\phi_1$  and  $\phi_2$  are attained, as in Figure 2a(ii). In our binodal studies both approaches yielded layered coexisting phases whose compositions were identical within the scatter.

Once the coexisting layers form, the two-plateau profile is determined (using one of the appropriate depth-profiling methods), and the absolute values of  $\phi_1$  and  $\phi_2$  are determined as described in more detail elsewhere.<sup>22</sup> It is also possible to monitor how the coexisting phase compositions vary with annealing time, to ensure that the equilibrium values have indeed been attained, as shown in Figure 2 for one of the polyolefin blend systems considered later.

For the case of the surface enrichment profiles, a layer at the required composition is spin-cast and annealed at the appropriate temperature in the one-phase region. When equilibrium is reached and the surface is enriched in the preferred phase (see Figure 1b), the sample is rapidly frozen to temperatures lower than its glass transition until the profiles are measured.

**$\chi_{AB}$  for Polyolefin Mixtures from Binodals.** Interaction parameters have been determined using the above approach for many binary pairs,<sup>11,18,20–22</sup> but here we consider only those cases where both depth profiling and SANS have been used on identical pairs. The polymers used in the binodal  $\chi_{AB}$  determination<sup>18,22</sup> were polyolefinic ethylene/ethylethylene (E/EE) copolymers, as shown in Table 1.

Composition–depth profiles of thin films of the mixtures d66/h52, d52/h66, and d78/h88 were used to generate binodals, as described in more detail elsewhere.<sup>22</sup> A typical binodal, for the d66/h52 blend, is reproduced in Figure 3.

To extract the interaction parameter from binodals,<sup>21,22</sup> such as in Figure 3, one starts with the Flory–Huggins functional for the normalized free energy of mixing  $\Delta F_M$  in a binary A/B mixture,<sup>35,36</sup>

$$\Delta F_M/k_B T = (\phi/N_A) \ln \phi + ((1 - \phi)/N_B) \ln(1 - \phi) + \phi(1 - \phi)\chi_{AB} \quad (1)$$

where subscripts label the A or B components (save that  $k_B$  is the Boltzmann constant), and  $\phi = \phi_A = (1 - \phi_B)$  ( $\phi_x$  here and throughout refers to volume fraction of species  $x$ ). Given a relation between  $\chi_{AB}$  and  $T$ , the binodal may readily be generated (for example, by the common tangent construction<sup>21</sup> which imposes equality of the chemical potential of the two coexisting phases at any  $T < T_c$ , the UCST). The reverse process, whereby

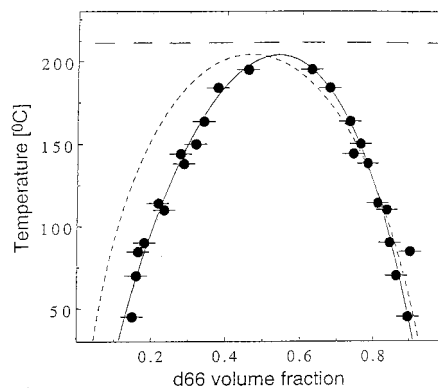


**Figure 3.** Phase-coexistence diagram for the d66/h52 blend, determined from composition–depth profiling of coexisting phases in thin films. The broken curve corresponds to a fit using the Flory–Huggins free energy of mixing with an interaction parameter of the form  $\chi = A/T$ , while the solid curve uses a form with a composition dependence,  $\chi_{AB} = [(A'/T) + B](1 + C\phi)$ , with values of the parameters as in Table 2. (The horizontal broken line at  $T = 210$  °C indicates that at that temperature full interdiffusion occurred for this pair. Adapted from ref 22.)

a parametric form is assumed for  $\chi_{AB}$  and the fit to the experimentally determined binodal optimizes the values of the parameters, is used in our case to extract the interaction parameter from the binodal data.<sup>21,22</sup> One may use the simplest form originally proposed by Flory,<sup>35,36</sup>  $\chi_{AB} = A/T$ , where  $A'$  is a constant, which assumes that only dispersive (van der Waals) interactions play a role. If this is done with the binodal in Figure 3, using appropriate values for  $A'$ , the broken curve shown in Figure 3 is predicted. Clearly such a form for  $\chi_{AB}$ , while qualitatively reproducing the main features of the binodal, is not fully satisfactory. In particular, it fails to predict the position of the critical composition. Similar comments apply for the binodals measured for the other mixtures.<sup>22</sup> A better fit is obtained when  $\chi_{AB}$  is allowed to have an entropic contribution and is also allowed to vary with composition  $\phi$ , as often suggested earlier.<sup>37</sup> To fit the binodals for the polyolefin mixtures in the present case, the simplest linear variation of  $\chi_{AB}$  with  $\phi$  was used,<sup>22</sup>

$$\chi_{AB} = [(A/T) + B](1 + C\phi) \quad (2)$$

This is found to provide a good fit to the experimental binodals, as exemplified by the solid curve for the example of d66/h52 in Figure 3. It should be noted that a parabolic variation of  $\chi$  with composition, of the form  $\chi_{AB} = [(A/T) + B]\{1 + C\phi(1 - \phi)\}$ , cannot be well fitted to the data, mainly because it cannot lead to the correct value of the critical composition. We return to this issue of the compositional variation of  $\chi$  in the following section. In Table 2 we give the composition-dependent form  $\chi_{AB} = [(A/T) + B](1 + C\phi)$ , taken from ref 22, for the best fit to the binodals for the three mixtures considered.

**$\chi_{AB}$  for Isotopic Polystyrene Blends from Surface-Segregation Profile.** When one of the components in a miscible binary mixture is preferentially attracted to a surface, it will segregate to that surface to form a surface layer enriched over the bulk composition  $\phi_\infty$  (schematically indicated in Figure 1b). The composition at the surface will be  $\phi_s > \phi_\infty$ , and mean-field theory<sup>38</sup> predicts a composition profile at a distance  $z$  from the enriched surface given by the implicit equation



**Table 2. Composition-Dependent Interaction Parameters<sup>a</sup>**

mixture	interaction parameter $\chi_{AB}(T, \phi)^b$
d66/h52	$(0.327/T + 3.48 \times 10^{-4})(1 + 0.222\phi)$
h66/d52	$(0.452/T - 1.2 \times 10^{-4})(1 + 0.031\phi)$
h88/d78	$(0.454/T - 9 \times 10^{-7})(1 + 0.064\phi)$

<sup>a</sup> The values of  $\chi_{AB}(T, \phi) = (A/T + B)(1 + C\phi)$  provide the best fit to the binodals measured for the blends used (see solid curve in example in Figure 3). <sup>b</sup> The  $\phi$ -dependence is with respect to the higher branched component in all cases (i.e., the d66, h66, and h88 components in the three mixtures). Adapted from ref 22.

$$z = \frac{a}{6} \int_{\phi=\phi_s}^{\phi=\phi(z)} \{ \phi(1-\phi)[\Delta F_M(\phi) - \Delta F_M(\phi_\infty) - \Delta\mu(\phi - \phi_\infty)] \}^{-1/2} d\phi \quad (3)$$

where  $a$  is the weighted statistical segment length of the polymers and  $\Delta\mu$  is the exchange chemical potential given by  $\Delta\mu = \partial\Delta F_M(\phi_\infty)/\partial\phi|_{\phi_\infty}$ . The best fit of the curve predicted by eq 3 to the experimental profile may then be used to extract  $\chi_{AB}$ , which appears in the expression for  $\Delta F_M$  (eq 1). The full predicted curve from eq 3 can be shown<sup>23</sup> to be very close to an exponentially decaying composition of the form

$$\phi(z) = \phi_\infty + (\phi_s - \phi_\infty)e^{-z/\xi_b} \quad (4)$$

where the enriched surface (air)  $\phi = \phi_s$  is at  $z = 0$  and the decay length  $\xi_b$  is the bulk correlation length. This is related to the interaction parameter  $\chi_{AB}$  as

$$\xi_b = \frac{a}{6} \left( \frac{1-\phi}{2N_A} + \frac{\phi}{2N_B} - \chi_{AB}\phi(1-\phi) \right)^{-1/2} \quad (5)$$

Thus, the value of  $\chi_{AB}$  may be determined from a fit of the enrichment profile to eq 4.

To compare  $\chi_{AB}$  from surface enrichment profiles with values extracted from SANS for identical blends, we examine the isotopic pair dPS/hPS,<sup>23</sup> for which the deuterated component is enriched at the air or vacuum surface. NRA with enhanced spatial resolution (in the proton detection mode) was used to determine the detailed shape of the near-surface composition profile<sup>23</sup> in such blends, for different molecular weights  $M$  and bulk compositions  $\phi_\infty$  at two different temperatures in the one-phase regime. The profiles are shown in Figure 4.

Also shown as solid curves in Figure 4 are the best fits of the predicted composition profiles based on eq 4, with the appropriate values of  $\chi_{AB}$  in eq 5, convoluted with a depth-dependent spatial resolution<sup>39</sup> corresponding to the NRA configuration used. The best fits were determined by evaluating the normalized sum dev of the square of the residuals, according to

$$\text{dev} = \frac{1}{n} \sum_i^n (\phi_i^{\text{fit}} - \phi_i^{\text{data}})^2 \quad (6)$$

where  $(\phi_i^{\text{fit}} - \phi_i^{\text{data}})$  is the deviation of the value of the measured volume fraction datum from the value given by fitting eq 4, and  $n$  is the total number of data points  $i$ . The variation of dev with  $\chi_{AB}$  is shown in the inset for each of the profiles in Figure 4. The value of  $\chi_{AB}$  corresponding to the best fit is that which minimizes dev (to a value dev<sub>min</sub>), while the uncertainties are estimated from the limits determined by  $\delta\text{dev}/\text{dev}_{\text{min}} = 0.1$ , shown as horizontal bars in the insets in Figure 4.

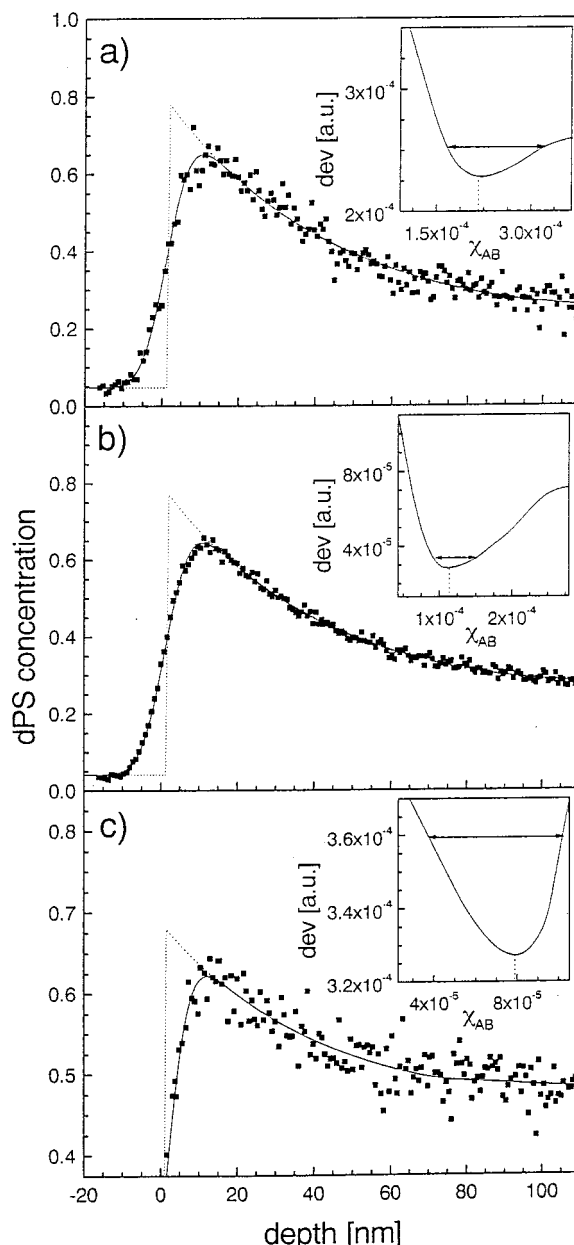


**Figure 4.** Surface enrichment profiles obtained via NRA at the air surface of thin films of isotopic hPS/dPS mixtures at temperatures  $T > T_c$ . (a) hPS ( $M = 1.15 \times 10^6$ )/dPS ( $M = 1.3 \times 10^6$ ) at  $T = 180$  °C,  $\phi_\infty = 0.33$ . (b) hPS ( $M = 1.95 \times 10^6$ )/dPS ( $M = 1.95 \times 10^6$ ) at  $T = 245$  °C,  $\phi_\infty = 0.30$ . (c) hPS ( $M = 1.95 \times 10^6$ )/dPS ( $M = 1.95 \times 10^6$ ) at  $T = 245$  °C,  $\phi_\infty = 0.50$ . The solid curves are best fits using eq 4 (dotted curve) convoluted with the depth-dependent spatial resolution of the NRA method, using the interaction parameter  $\chi_{AB}$  corresponding to the minimum in the dev (normalized sum of residuals) vs  $\chi_{AB}$  plots shown in the inset to each profile. The bar in each dev plot is the estimated uncertainty in the best-fit  $\chi_{AB}$  (profiles (a) and (b) adapted from ref 23).

The best fit values extracted using this procedure are  $\chi_{AB} = 2.16_{-0.5}^{+1.0} \times 10^{-4}$  at  $T = 180$  °C,  $\phi_{\infty\text{dPS}} = 0.33$  (Figure 4a);  $\chi_{AB} = 1.13_{-0.2}^{+0.4} \times 10^{-4}$  at  $T = 245$  °C,  $\phi_{\infty\text{dPS}} = 0.30$  (Figure 4b); and  $\chi_{AB} = 0.79_{-0.4}^{+0.2} \times 10^{-4}$  at  $T = 245$  °C,  $\phi_{\infty\text{dPS}} = 0.5$  (Figure 4c).

### 3. Comparison with Interaction Parameters Determined by SANS

**Polyolefin Blends.** SANS has been widely used to determine interaction parameters in blends of high

molecular weight binary polymer mixtures in the one-phase regime.<sup>40–45</sup> In this approach the wavenumber ( $q$ )-dependent structure factor  $S(q)$  is related to the interaction parameter via the random-phase approximation due to de Gennes.<sup>36</sup> It may be written<sup>44</sup> as

$$S^{-1}(q) = \{N_A \phi v_A P_A(q)\}^{-1} + \{N_B (1 - \phi) v_B P_B(q)\}^{-1} - (2/v) \chi_{\text{SANS}} \quad (7)$$

where  $N_A$  and  $N_B$  are the degrees of polymerization of the chains of polymers A and B, respectively,  $\phi$  is the volume fraction of species A, and the bulk mixture is assumed incompressible.  $v_i$  and  $P_i$  are the monomeric volumes and scattering form factors of the individual components, and  $v$  is a reference volume (often chosen as  $(v_A v_B)^{1/2}$  for convenience). The interaction parameter is written as  $\chi_{\text{SANS}}$  to indicate that it is derived from the SANS measurements in accord with eq 7 and differs from the traditionally defined  $\chi_{\text{AB}}$  appearing in the usual expression for the Flory–Huggins free energy of mixing  $\Delta F_M$  in eq 1. The two are related as

$$\chi_{\text{SANS}} = -(1/2) \partial^2(\phi(1 - \phi)\chi_{\text{AB}})/\partial^2\phi \quad (8)$$

For a composition-dependent interaction parameter as extracted for the polyolefin blends,  $\chi = [(A/T) + B](1 + C\phi)$  (where the values of  $A$ ,  $B$ , and  $C$  are given in Table 2), substitution in eq 8 yields

$$-(1/2) \partial^2(\phi(1 - \phi)\chi)/\partial^2\phi = [(A/T) + B](1 - C + 3C\phi) \quad (9)$$

Values of  $\chi_{\text{SANS}}$  as a function of blend composition at different temperatures for the blends d52/h66, d66/h52, and d78/h88 studied by NRA have been reported by Krishnamoorti et al.<sup>44</sup> These data are reproduced from the original paper<sup>44</sup> in Figures 5–7, where they are compared, via eq 9, with the interaction parameters determined using the binodals as described in the previous section, with the values of the parameters appearing in Table 2.

From Figures 5–7 we see that the agreement of  $\chi$  extracted using the binodals with the values based on SANS is essentially quantitative. A closer examination reveals several important points. Over the middle of the composition range (25–75%), for all three blends and at all temperatures, the binodally extracted  $\chi$  differs from  $\chi_{\text{SANS}}$  by some 20–25% at most, and generally by 10% or even less, differences that are within the uncertainty in the data. It is of especial interest—in view of the linear  $\phi$  variation assumed for  $\chi$  in fitting the coexistence data—that in all cases the variation of the interaction parameter with composition deduced from the binodals, though weak in some cases, is in the same sense and of very similar magnitude as that indicated by the SANS data in the midrange composition region. Thus, for the 66/52 blends,  $\chi$  increases in both cases with concentration of the 66 component, whether deuterated or protonated, while for the h88/d78 blend  $\chi$  increases with the h88 volume fraction. Precisely this variation is indicated in the composition midrange regime also by the SANS data. We conclude that over most of the composition range the interaction parameters deduced from fitting to the binodal and from SANS are in very good qualitative and quantitative agreement with each other.

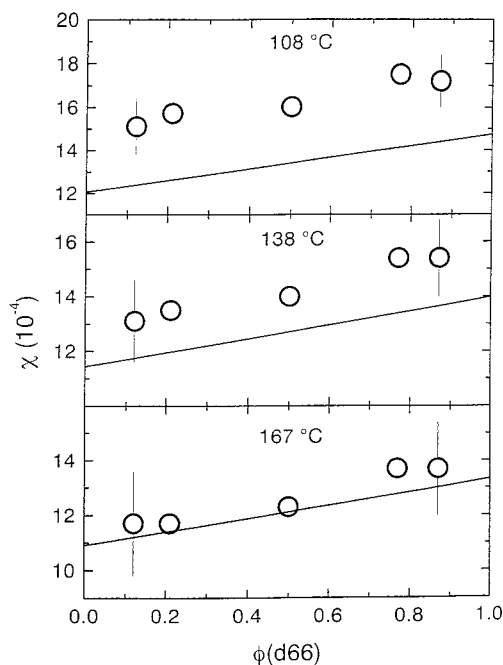


**Figure 5.** Comparison of composition-dependent interaction parameter  $\chi_{\text{AB}}$  obtained from fitting to binodals determined by NRA composition–depth profiling (solid lines, from Table 2), with values obtained by Krishnamoorti et al.<sup>44</sup> using SANS (open circles), for the binary mixture d66/h52 at the temperatures shown.

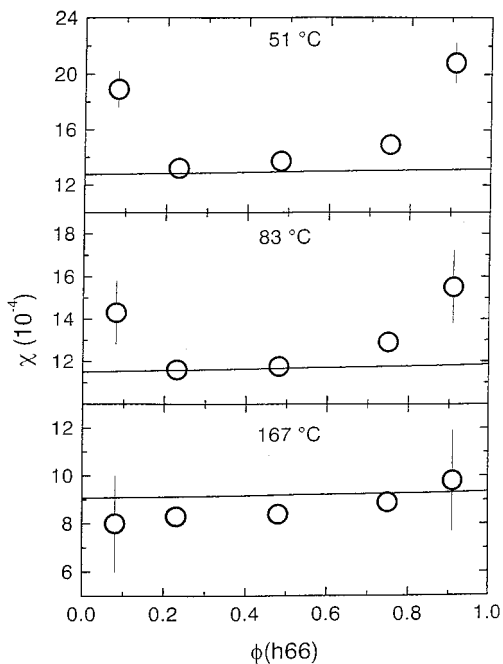


**Figure 6.** As in Figure 5, for the mixture h66/d52.

Finally, we should note that at the extremes of the composition range the SANS data<sup>44</sup> for some of the mixtures and temperatures compared (especially for the d52/h66 blend, Figure 6 top) show an upturn, suggesting a parabolic variation of  $\chi_{\text{SANS}}$  with  $\phi$ . Such a variation has also been observed in  $\chi_{\text{SANS}}$  for other polyolefin blends<sup>44</sup> (not shown) but is clearly not manifested in the binodally deduced  $\chi$ : we recall—see previous section—that a parabolic form for  $\chi$  could not result in a satisfactory fit to the binodals. While it is beyond the scope of the present paper to consider the possible origins of this “parabolic” effect, or of other factors

Table 3

study	functional form	$T = 453 \text{ K}, \phi = 33\%$	$T = 518 \text{ K}, \phi = 30\%$	$T = 518 \text{ K}, \phi = 50\%$
Bates and Wignall <sup>40</sup> (SANS)	$\chi(T) = (0.20 \pm 0.01)/T - (2.9 \pm 0.5) \times 10^{-4}$	$(1.52 \pm 0.54) \times 10^{-4}$	$(0.96 \pm 0.54) \times 10^{-4}$	$(0.96 \pm 0.54) \times 10^{-4}$
Schwahn et al. <sup>42</sup> (SANS)	$\chi(T) = (0.28 \pm 0.02)/T - (4.9 \pm 0.5) \times 10^{-4}$	$(1.28 \pm 0.64) \times 10^{-4}$	$(0.51 \pm 0.64) \times 10^{-4}$	$(0.51 \pm 0.64) \times 10^{-4}$
this study (NRA, surface enrichment)		$2.16_{-0.5}^{+1.0} \times 10^{-4}$	$1.13_{-0.2}^{+0.4} \times 10^{-4}$	$0.79_{-0.4}^{+0.2} \times 10^{-4}$

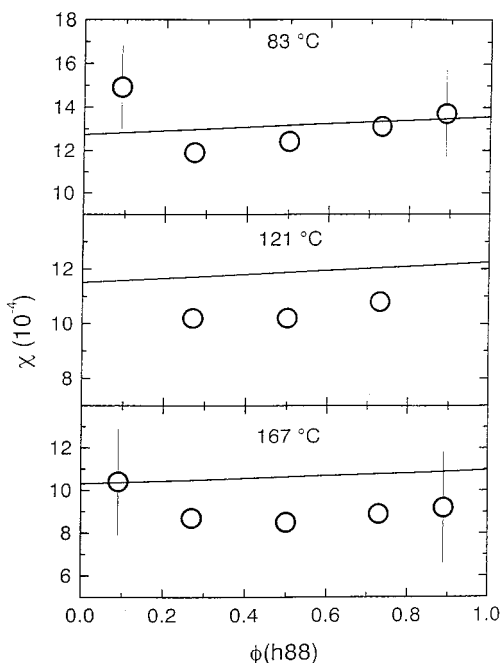


Figure 7. As in Figure 5, for the mixture h88/d78.

leading to a composition dependence<sup>37,46–52</sup> of  $\chi$ , we note that the variation of  $\chi_{\text{SANS}}(\phi)$ , particularly the upturn at the extremes of the composition, has recently been discussed by Taylor-Maranas et al.<sup>45</sup> These authors analyze compressibility effects on neutron scattering by polymer blends in some detail, and conclude that the “reality of the parabolic concentration dependence [of  $\chi_{\text{SANS}}$ ] must be considered an open question”. This opens the possibility that the linear dependence of the interaction parameter, as deduced from the binodals and from SANS in the composition midrange, may in fact describe the interaction behavior also at the extremes of the composition for these polyolefin systems.

**Isotopic Polystyrene Mixtures.** SANS studies of hPS/dPS isotopic mixtures have been reported by Bates and Wignall<sup>40</sup> and by Schwahn and co-workers.<sup>42</sup> In Table 3 we compare our results from the surface enrichment profiles with these SANS values.<sup>53</sup> At both temperatures the values of the interaction parameter derived from the surface enrichment profiles are close to the mean values extracted from the independent SANS studies and well within the quoted uncertainties in the latter. (We note that these rather large quoted uncertainties derive not from scatter in the SANS data, but rather from uncertainties in the absolute scattering intensities measured.)

#### 4. Discussion and Conclusions

Our main findings are that segmental interaction parameters in polymer blends, extracted from binodals and surface enrichment in thin films, are in good quantitative agreement with those extracted from the identical blends from SANS together with RPA. In what follows we make some remarks concerning the general-

ity and limitations of the thin-film depth-profiling approach—in determination of binodals and surface enrichment profiles—as an alternative to SANS for extracting  $\chi$  parameters in high polymer mixtures.

The composition–depth profiles of phase-separated polymer films can yield, in principle, the most direct measure of the binodal. However, the ion beam cross section, both in ion beam methods and in other techniques such as SIMS, is relatively large, and lateral resolution is no better than tens of micrometers to millimeters with these methods (as opposed to depth resolution which is a few nanometers). Thus, in determining the coexistence profiles, it is implicitly assumed that the two phases layer parallel to the underlying substrate, as indicated in Figure 1a (bottom). While this has been the case with the mixtures studied to date, it is in fact possible to promote this more generally by creating the appropriate confining surfaces for the mixture film, so that one surface prefers the A phase while the other prefers the B phase. This may be done, for example, by spin-casting a layer of one of the pure components (A say) onto the underlying solid substrate (typically polished silicon or gold-coated silicon wafers) and lightly cross-linking it in a defocused ion beam.<sup>54</sup> This creates a “frozen” surface coating of the A component and promotes the likelihood that it will be preferred—for enthalpic reasons—by the A-rich phase when the phases undergo separation. Similarly, a lightly cross-linked B layer may be floated onto the top of the film, promoting preferment at that interface by the B-rich phase. Preliminary measurements have indicated the feasibility of the cross-linking procedure. In this way the layering geometry illustrated in Figure 1a (bottom) may be induced systematically.

As noted, use of thin films is mandated if equilibrium coexistence or surface enrichment profiles are to be attained in reasonable times. The question arises whether the binodals themselves depend on the finite film thickness. This issue has recently been addressed both theoretically and experimentally. Theoretically, one expects that, for film thicknesses beyond some  $20\xi_b$ , where  $\xi_b$  is the bulk correlation length and is of order 10 nm in typical cases, finite size effects on the binodals should be negligible.<sup>55</sup> In practice, for the systems used this corresponds to values of order 300 nm, and in the binodal studies above film thicknesses were always in excess of this. Moreover, in a very recent study of the effects of film thickness on interfacial widths between coexisting phases,<sup>19,39</sup> the coexisting compositions did not vary (within the scatter) over the film thickness range 300–1400 nm. We conclude that in practical situations the effects of finite film thickness on the binodals may readily be eliminated.

A further issue concerns the smoothness of the surfaces in the surface enrichment determination, which may be rougher than the underlying substrates due to capillary waves, for example. Studies on films of differing thickness have shown clearly that the effective width of the interface between two coexisting phases parallel to the film plane can vary strongly with film



thickness.<sup>19,39</sup> This is due to capillary waves at the interphase boundary and can be much larger than the intrinsic width expected from mean-field theory. However, these capillary waves are large because of the weak surface tension between the coexisting phases. In contrast, the surface tension at the polymer/air surface is very much larger, so that capillary waves at that interface have a very low amplitude. Thus, the air surface, as also revealed directly by AFM measurements,<sup>54</sup> is very smooth (rms roughness around 2 nm or less) and has little effect on the measured enrichment profile.

Another question concerns the applicability of mean-field models to analysis of the profiles. While at temperatures  $T < T_c$  not too near the critical point the coexistence curves are expected to obey well the mean-field models in the case of high molecular weight mixtures, care must be taken with the surface enrichment profiles. This is because the Cahn–Hilliard-type analysis used to fit the data assumes a slow variation of the compositional variation, requiring  $a^2(\nabla\phi)^2 \ll N^{-1}$ . In practice, for the high- $M$  isotopic mixture described in section 3.2, this is well obeyed,<sup>23</sup> so that the mean-field results due to Schmidt and Binder<sup>38</sup> are expected to hold well, and this has been explicitly shown for the hPS/dPS mixtures described.<sup>23</sup>

We conclude that an approach to measuring interaction parameters in polymer mixtures that is based on composition–depth profiling in thin films can be a convenient, rapid, and accurate alternative to SANS in many cases. This is because thin-film depth profiling requires experimental tools that are more readily accessible than the neutron sources essential for SANS. The main requirement is a capability for directly profiling the thin-film composition. For the systems described above we employed NRA, using a small (3 MV) Van de Graaff accelerator, but other convenient approaches are readily available, most notably dynamic SIMS<sup>10,28,29</sup> and FRES<sup>3,5,25–27</sup> and have been used extensively in several laboratories in recent years. The need to label the samples with deuterium is one common also to the neutron scattering studies and has been successfully addressed in a wide range of polymers. Finally, the fact that only minute quantities of material for carrying out the measurements are required (of order 100 mg or less of each component for a complete binodal determination) is also an attractive feature of this approach.

**Acknowledgment.** We thank Kurt Binder for useful discussions and suggestions. The Ministry of Sciences and Arts (Tashtiot program), the German–Israel Foundation (GIF), and the US–Israel Binational Science Foundation are gratefully acknowledged for their support.

## References and Notes

- (1) Kramer, E. J.; Green, P. F.; Palmstrom, C. J. *Makromol. Chem. Rapid Commun.* **1984**, *5*, 159.
- (2) Mills, P. F.; Green, P. F.; Palmstrom, C. J.; Mayer, J. W.; Kramer, E. J. *Appl. Phys. Lett.* **1984**, *45*, 958.
- (3) Green, P. F.; Doyle, B. L. *Phys. Rev. Lett.* **1986**, *57*, 2407.
- (4) Klein, J. *Science* **1990**, *250*, 640.
- (5) Composto, R. J.; Kramer, E. J.; White, D. M. *Nature* **1987**, *328*, 234.
- (6) Crist, B.; Green, P. F.; Jones, R. A. L.; Kramer, E. J. *Macromolecules* **1989**, *22*, 2857.
- (7) Losch, A.; Salomonovic, R.; Steiner, U.; Fetters, L. J.; Klein, J. *J. Polym. Sci., Polym. Phys.* **1995**, *33*, 1821.
- (8) Jones, R. L.; Kramer, E. J.; Rafailovich, M. H.; Sokolov, J.; Schwarz, S. A. *Phys. Rev. Lett.* **1989**, *62*, 280.
- (9) Jones, R. A. L.; Norton, L. J.; Kramer, E. J.; Composto, R. J.; Stein, R. S.; Russell, T. P.; Mansour, A.; Karim, A.; Fletcher, G. P.; Rafailovich, M. H.; Sokolov, J.; Zaho, X.; Schwarz, S. A. *Europhys. Lett.* **1990**, *12*, 41.
- (10) Zhao, X.; Zhao, W.; Sokolov, J.; Rafailovich, M. H.; Schwarz, S. A.; Wilkens, B. J.; Jones, R. A. L.; Kramer, E. J. *Macromolecules* **1991**, *24*, 5991.
- (11) Steiner, U.; Klein, J.; Eiser, E.; Budkowski, A.; Fetters, L. J. *Science* **1992**, *258*, 1126.
- (12) Bruder, F.; Brenn, R. *Europhys. Lett.* **1993**, *22*, 707.
- (13) Scheffold, F.; Budkowski, A.; Steiner, U.; Eiser, E.; Klein, J.; Fetters, L. J. *J. Chem. Phys.* **1996**, *104*, 8795.
- (14) Jones, R. A. L.; Norton, L. J.; Kramer, E. J.; Bates, F. S.; Wiltzius, P. *Phys. Rev. Lett.* **1991**, *66*.
- (15) Krausch, G.; Dai, C.-A.; Kramer, E. J.; Marko, J. F.; Bates, F. *Macromolecules* **1993**, *26*, 5566.
- (16) Chaturvedi, U. K.; Steiner, U.; Zak, O.; Krausch, G.; Klein, J. *Phys. Rev. Lett.* **1989**, *63*, 616.
- (17) Steiner, U.; Krausch, G.; Schatz, G.; Klein, J. *Phys. Rev. Lett.* **1990**, *64*, 1119.
- (18) Eiser, E.; Budkowski, A.; Steiner, U.; Klein, J.; Fetters, L. J.; Krishnamoorti, R. *ACS PMSE Proc.* **1993**, *69*, 176.
- (19) Kerle, T.; Klein, J.; Binder, K. *Phys. Rev. Lett.* **1996**, *77*, 1318.
- (20) Bruder, F.; Brenn, R. *Macromolecules* **1991**, *24*, 5552.
- (21) Budkowski, A.; Steiner, U.; Klein, J.; Schatz, G. *Europhys. Lett.* **1992**, *18*, 705.
- (22) Scheffold, F.; Eiser, E.; Budkowski, A.; Steiner, U.; Klein, J.; Fetters, L. J. *J. Chem. Phys.* **1996**, *104*, 8786.
- (23) Zink, F.; Kerle, T.; Klein, J. *Macromolecules* **1998**, *31*, 417.
- (24) Green, P. F.; Kramer, E. J. *J. Mater. Res.* **1986**, *1*, 202.
- (25) Sokolov, J.; Rafailovich, M. H.; Jones, R. A. L.; Kramer, E. J. *Appl. Phys. Lett.* **1989**, *54*, 590.
- (26) Shull, K. R.; Kramer, E. J.; Hadziioannou, G.; Tang, W. *Macromolecules* **1990**, *23*, 4780.
- (27) Genzer, J.; Rothman, J. B.; Composto, R. J. *Nucl. Instrum. Methods Phys. Res.* **1994**, *B86*, 345.
- (28) Whitlow, S. J.; Wool, R. P. *Macromolecules* **1989**, *22*, 2648.
- (29) Schwarz, S. A.; Wilkens, B. J.; Pudensi, M. A. A.; Rafailovich, M. H.; Sokolov, J.; Zhao, X.; Zhao, W.; Zheng, X.; Russell, T.; Jones, R. A. L. *Mol. Phys.* **1992**, *76*, 937.
- (30) Giessler, K.-H.; Endisch, F.; Rauch, F.; Stamm, M. *Fresenius' J. Anal. Chem.* **1993**, *346*, 151.
- (31) Chaturvedi, U.K.; Steiner, U.; Zak, O.; Krausch, G.; Schatz, G.; Klein, J. *Appl. Phys. Lett.* **1990**, *56*, 1228.
- (32) Budkowski, A.; Steiner, U.; Klein, J. *J. Chem. Phys.* **1992**, *97*, 5229.
- (33) Yerushalmi-Rozen, R.; Klein, J. *Science* **1994**, *263*, 793.
- (34) Kerle, T.; Scheffold, F.; Losch, A.; Steiner, U.; Schatz, G.; Klein, J. *Acta Polym.* **1997**, *48*, 548.
- (35) Flory, P. *Principles of Polymer Chemistry*; Cornell University Press: Ithaca, NY, 1971.
- (36) de Gennes, P. G. *Scaling Concepts in Polymer Physics*; Cornell University Press: London, 1979.
- (37) For some discussion of earlier work on the composition dependence of the segmental interaction interaction parameters, see for example ref 45 and papers cited therein.
- (38) Schmidt, I.; Binder, K. *J. Phys. (Paris)* **1985**, *46*, 1631.
- (39) Kerle, T.; Klein, J.; Binder, K. *Eur. Phys. J.* **1999**, *B7*, 401.
- (40) Bates, F. S.; Wignall, G. D. *Phys. Rev. Lett.* **1986**, *57*, 1429.
- (41) Jinnai, H.; Hasegawa, H.; Hashimoto, T.; Briber, R. M.; Han, C. C. *Macromolecules* **1993**, *26*, 182.
- (42) Schwahn, D.; Hahn, K.; Treib, J.; Springer, T. *J. Chem. Phys.* **1990**, *93*, 8383.
- (43) Balsara, N. P.; Fetters, L. J.; Hadjichristidis, N.; Lohse, D. J.; Hahn, C. C.; Graessley, W. W.; Krishnamoorti, R. *Macromolecules* **1992**, *25*, 6137.
- (44) Krishnamoorti, R.; Graessley, W. W.; Balsara, N. P.; Lohse, D. J. *J. Chem. Phys.* **1994**, *100*, 3894.
- (45) Taylor-Maranas, J. K.; Debenedetti, P. G.; Graessley, W. W.; Kumar, S. K. *Macromolecules* **1997**, *22*, 66943.
- (46) See: Koningsveld, R.; Kleintjens, L. A.; Nies, E. *Croat. Chem. Acta* **1987**, *60*, 53 for a review to about 1986.
- (47) Binder, K. *Colloid Polym. Sci.* **1988**, *266*, 871.
- (48) Bates, F. S.; Schulz, M. F.; Rosendale, J. H. *Macromolecules* **1992**, *25*, 5547.
- (49) Schweitzer, K. S. *Macromolecules* **1993**, *26*, 6050.
- (50) Kumar, S. N. *Macromolecules* **1994**, *27*, 260.
- (51) Dudowicz, J.; Freed, K. *J. Chem. Phys.* **1992**, *96*, 9147.
- (52) Liu, A. J.; Fredrickson, G. H. *Macromolecules* **1994**, *27*, 2503.
- (53) Bates, F. S.; Fredrickson, G. H. *Macromolecules* **1994**, *27*, 1065.

(53) We do not consider for the isotopic mixtures the issue of compositional dependence of the interaction parameter. Such a dependence for the PS/dPS mixture was examined by Schwahn et al.<sup>42</sup> (but not by Bates and Wignall<sup>40</sup>), who also however presented a composition-independent form for  $\chi_{\text{SANS}}$ , which is the one quoted in Table 3. At the compositions reported (Figure 4) the composition-dependent SANS values of Schwahn et al. are close to the values given in Table 3. (A

composition-dependent value of  $\chi_{\text{AB}}$  was reported by Budkowski et al.<sup>21</sup> based on a fit to the PS/dPS binodal; the values are within the estimated uncertainty of those in Table 3.)

(54) Kerle, T.; Yerushalmi-Rozen, R.; Klein, J. *Macromolecules* **1998**, *31*, 422.

(55) Flebbe, T.; Duenweg, B.; Binder, K. *J. Phys. II* **1995**, *6*, 667.

MA990798A